DO ENVIRONMENTAL MARKETS CAUSE ENVIRONMENTAL INJUSTICE?
EVIDENCE FROM CALIFORNIA'S CARBON MARKET

Danae Hernandez-Cortes
Kyle C. Meng

Do Environmental Markets Cause Environmental Injustice? Evidence from California's Carbon
Market
Danae Hernandez-Cortes and Kyle C. Meng
NBER Working Paper No. 27205
May 2020
JEL No. H4,I14,Q5,Q51,Q52,Q53,Q54

ABSTRACT

Market-based environmental policies are widely adopted on the basis of allocative efficiency. However, there is a growing distributional concern that market forces could increase the pollution exposure gap between disadvantaged and other communities by spatially reallocating pollution. We estimate how this "environmental justice gap" changed following the 2013 introduction of California's carbon market, the world's second largest and the one most subjected to environmental justice critiques. Embedding a pollution transport model within a program evaluation framework, we find that while the EJ gap was widening prior to 2013, it has since fallen by 21-30% across pollutants due to the policy.

Danae Hernandez-Cortes
Department of Economics
University of California, Santa Barbara
Santa Barbara, CA 93106
hernandezcortes@umail.ucsb.edu

Kyle C. Meng
Bren School of Environmental
Science and Management
Department of Economics
University of California, Santa Barbara
4416 Bren Hall
Santa Barbara, CA 93106
and NBER
kmeng@bren.ucsb.edu

1 Introduction

Market-based environmental policies - such as pollution trading and taxes - have been increasingly used to address environmental problems. Today, these policies cover 30% of global fisheries (Costello et al., 2016), account for over $36 billion in global ecosystem service payments (Salzman et al., 2018), and govern 20% of global greenhouse gas (GHG) emissions (World Bank Group, 2019).

The central appeal of market-based policies is allocative efficiency. The price on pollution introduced by these policies reduces the aggregate cost of meeting an environmental objective by inducing less abatement from polluters with high marginal abatement cost (Dales, 1968; Montgomery, 1972). This stands in contrast with more costly command-and-control regulations, which require heterogeneous polluters to adopt uniform abatement actions.

The reallocation induced by market-based policies also spatially alters where pollution occurs and thus who are harmed by it. In particular, the gap in pollution exposure between disadvantaged and other communities - already large in many settings[1] - could potentially widen following the introduction of a market-based policy (Chinn, 1999; Corburn, 2001; Ringquist, 2011; Fowlie, Holland and Mansur, 2012).

In recent years, there has been increasing opposition to market-based policies because of this environmental justice (EJ) concern, which has in some settings overtaken efficiency arguments. For example, recent efforts to introduce state-level U.S. climate policies and renew the European Union Emissions Trading System were opposed on EJ grounds (Leber, 2016; Herron, 2019; Transnational Institute, 2013). EJ opposition has been particularly prominent in the case of California's GHG cap-and-trade (C&T) program, the world's second largest, and arguably most ambitious, carbon market. EJ concerns led to a temporary pause in the program's development in 2011 (Takade, 2013) and nearly halted renewal efforts in 2017 (Megerian, 2017). Unfortunately, the debate in California has occurred largely in the absence of causal evidence.

Whether a market-based environmental policy widens or narrows the pollution exposure gap between disadvantaged and other communities, henceforth the "EJ gap," depends on the spatial distribution of polluters, their abatement costs, and the location of disadvantaged communities. A market-based policy induces relatively less pollution abatement from high marginal abatement cost polluters. If disadvantaged communities, which are typically exposed to higher baseline levels of pollution, are downwind of these polluters, a market-based policy will widen the EJ gap. But if other communities are downwind of these polluters, the

---

[1]It is well documented that communities of lower income, greater minority share, and otherwise disadvantaged, are exposed to higher pollution levels than other communities (Bullard, 2000; Bowen, 2002; Ringquist, 2005; Mohai, Pellow and Roberts, 2009; Banzhaf, Ma and Timmins, 2019)

EJ gap will narrow (Burtraw et al., 2005; Fowlie, Holland and Mansur, 2012). Additionally, for a market-based policy regulating global pollutants like GHGs, the EJ gap effect depends on the relationship between GHG and local pollution emissions.

This paper provides novel causal evidence that California's GHG C&T program has reduced the EJ gap in NO_x, SO_x, $PM_{2.5}$, and PM_{10} following its 2013 introduction. We detect a large effect: the EJ gap, which was previously rising prior to 2013, has slowed so much because of the program that it is now falling. Between 2012 and 2017, the EJ gap fell by 21-30% across pollutants.

To detect this causal effect, we develop an empirical approach that overcomes two challenges found in prior work. The first challenge is to establish how a market-based policy causes a change in pollution emissions. Cross-sectional studies that correlate demographic characteristics with emissions or the presence of nearby polluting facilities have trouble discerning between pre-policy emission patterns from changes induced by the policy (Corburn, 2001; Ringquist, 2011; Cushing et al., 2018). We follow a recent economics literature by using a difference-in-difference research design to estimate how California's C&T program differentially affected emissions between regulated and unregulated facilities (Fowlie, Holland and Mansur, 2012; Grainger and Ruangmas, 2018; Meng, 2019; Walch, 2019; Mansur and Sheriff, 2019).

The second challenge involves determining how facility-level pollution *emissions* map onto location-specific pollution *exposure*, which matters ultimately for health outcomes. Prior literature typically assumes a facility's emissions disperse only within the same geographic unit (a.k.a. a unit-hazard coincidence) or within a distance circle centered around that facility (a.k.a. a distance-based measure) (Banzhaf, Ma and Timmins, 2019). These approaches, however, overlook the complex physical nature of pollution dispersal which, depending on atmospheric conditions and topography, can transport pollution from different sources and at different times in varying directions and distances. Failure to accurately account for pollution dispersal lead to treatment spillovers that can bias estimates even in otherwise valid quasi-experimental settings (Deschenes and Meng, 2018).

We address these challenges by explicitly embedding a pollution transport model within a program evaluation framework. First, we exploit the unique facility eligibility criteria and timing of California's GHG C&T program to isolate C&T-driven NO_x, SO_x, $PM_{2.5}$, and PM_{10} emissions during 2008-2017 from roughly 300 regulated stationary facilities.[2] Next, we insert C&T-driven emissions into a pollution transport model to determine how atmo-

---

[2]We consider only pollution exposure from C&T-regulated stationary sources in the electricity and industrial sectors because the program does not directly regulate or monitor emissions from non-stationary sources such as vehicles.

spheric and topographical conditions disperse C&T-driven emissions across California and over time. This computationally-intensive procedure involves generating over 11 million particle trajectories over our sample period. Finally, we use pollution exposure obtained from the transport model to examine changes in the C&T-driven pollution exposure gap between disadvantaged and other communities before and after the program's introduction.

We demonstrate that the EJ effect is insensitive to various robustness checks. These include using more flexible regression models; accounting for the closure of a major nuclear power plant in 2013; and using an alternative pollution transport model to incorporate atmospheric chemistry and secondary pollutants. The EJ effect, however, is sensitive to whether one fully models pollution dispersal. In particular, we show that employing more conventional approaches for assigning pollution exposure from emissions such as restricting exposure to only within an emitting facility's zip code or a distance circle centered around that facility results in considerably noisier and smaller EJ effects, consistent with bias occurring in the presence of pollution spillovers.

Finally, this paper's integration of program evaluation econometric techniques with pollution transport modeling can be applied more broadly. Nearly every effort to value the benefits of environmental policy must determine which locations are affected by changes in pollution emissions. Our empirical approach provides a path forward for addressing this widespread identification challenge found in the environmental valuation literature (Greenstone and Gayer, 2009; Graff Zivin and Neidell, 2013; Deschenes and Meng, 2018).

2   California's cap-and-trade program

California's climate policy is one of the world's most sophisticated and ambitious. In 2006, California passed Assembly Bill 32 (AB 32), requiring state-wide GHG emissions to reach 1990 emissions level by 2020. AB 32 was, and remains, the first of its kind: all other climate policies in the U.S. (state or national) regulate specific sectors, whereas AB 32 covers all GHG emission sources in California. The centerpiece of AB 32 was a cap-and-trade program, introduced in 2013 and administered by the California Air Resources Board (CARB). The program sets a limit, or cap, on total annual emissions. This limit is imposed through the issuance of a fixed supply of tradable emission permits. Regulated facilities are then either given or must purchase permits to cover annual emissions. The result is that regulated facilities face a price on their GHG emissions.

California's C&T program is now the world's second largest carbon market by value of permits, following the European Union Emissions Trading System. Not only has there been full compliance with the cap, but falling state-wide GHG emissions allowed California to

meet AB 32's 2020 target four years early in 2016. In 2016, California extended the state-wide GHG target to 40% below 1990 levels by 2030. The following year, the C&T program was also extended to 2030.

The C&T program has a unique eligibility requirement for regulated facilities. The program requires participation by all stationary GHG-emitting facilities producing at least 25,000 metric tons of annual carbon dioxide equivalent emissions, or CO_2e.[3] This eligibility criteria, which has been unchanged since 2013, covers all sectors that directly emit GHGs from stationary sources, including electricity and industrial sectors.[4] We use the facility eligibility criteria and the 2013 introduction of the GHG C&T program to isolate stationary, facility-level, local air pollution emissions driven by the program.[5] It should be noted that the GHG C&T program does not directly regulate emissions of local criteria air pollutants, such as NO_x, SO_x, $PM_{2.5}$, and PM_{10}. Any changes in the spatial distribution of local air pollution exposure due to the GHG C&T program is thus driven by the program's reallocation of GHG emissions and the co-production of local air pollutants with GHGs.

3   Data

Our analysis involves two primary datasets: 1) emissions of criteria air pollutants at the facility-by-year level and 2) a legal definition of a "disadvantage" community at the zip code level.

Air pollution emissions   We obtain 2008-2017 facility-level annual emissions of NO_x, SO_x, $PM_{2.5}$, and PM_{10} from CARB's Pollution Mapping Tool.[6] Stationary facilities with annual emissions past a certain threshold must report emissions to CARB. For NO_x, SO_x, $PM_{2.5}$, and PM_{10}, the reporting threshold is 10 metric tons per year. For GHGs, the reporting threshold is 10,000 metric tons of CO_2e. Because the CARB GHG reporting threshold is below the C&T program's eligibility threshold of 25,000 metric tons of CO_2e, we observe

---

[3]Greenhouse gases covered by the program were CO_2, CH_4, N_2O, HFCs, PFCs, SF6, NF3 and other fluorinated GHGs.

[4]In 2015, the GHG cap-and-trade program further covered suppliers of oil and natural gas using the same 25,000 metric ton of CO_2 equivalent criteria. Because fuel suppliers do not directly contribute to stationary GHG emissions, they are regulated based on the GHG content of their fuels (i.e., embedded carbon) which converts to GHG emissions when the fuel is eventually combusted from non-stationary sources (i.e., vehicles). We exclude fuel suppliers from our analysis because they do not directly produce or report GHG emissions.

[5]CARB also developed other regulations to meet the AB 32 target, such as a Low Carbon Fuel Standard and Advanced Clean Car Standards. These programs, however, were not market-based, were mostly introduced prior to 2012, and did not have the same facility-level eligibility criteria as the cap-and-trade program. Thus, while our estimated C&T effects take place in the presence of these other regulations, it is unlikely that C&T effects are conflated with the effects of these other regulations.

[6]Available here: https://ww3.arb.ca.gov/ei/tools/pollution_map/

NO$_x$, SO$_x$, PM$_{2.5}$, and PM$_{10}$ emissions for both GHG C&T-regulated and non-regulated stationary facilities. Both local criteria and GHG emissions are required to be reported annually by CARB.[7] Table S1 shows the number of GHG C&T regulated and non-regulated facilities in our sample and the distribution across sectors.[8] Each regulated facility is shown as a black dot in Figure 1a.

Several additional facility-level variables serve as input into the pollution transport model. CARB provides facility latitude and longitude as well as pollution-specific stack heights for a subset of facilities. For other facilities, we impute missing pollution-specific stack heights using sector averages constructed from non-missing observations.

Zip code definition of a disadvantaged community There is no established definition of a "disadvantaged" community. Previous papers in other empirical settings use a location's median income or minority share of population as proxy measures (Fowlie, Holland and Mansur, 2012; Grainger and Ruangmas, 2018; Mansur and Sheriff, 2019). For our setting, we use a legal definition of a "disadvantaged" community that has direct policy relevance. Senate Bill 535 (SB 535), passed in 2012, requires a portion of the revenue from the auction of C&T permits to be directed towards benefiting disadvantaged communities. To implement this spending, SB 535 formally defines a "disadvantaged community" using CalEnviroScreen, a fixed scoring system based on multiple indicators developed by the California Environmental Protection Agency. Specifically, a zip code is considered disadvantaged if it contains all or part of a census tract with a CalEnviroScreen score above the top 25th percentile. Zip codes designated as disadvantaged are shaded in dark blue in Figure 1a. Importantly, pre-2013 data was used in constructing CalEnviroScreen, which mitigates the concern that the introduction of cap-and-trade may have affected whether a zip code is designated as disadvantaged. We follow this definition because it is the basis for which zip codes receive government funds to offset environmental justice concerns. We further augment our zip code level data with average 2008-2012 population obtained from the U.S. Census Bureau.

---

[7] Details on CARB's reporting requirements can be found here: https://ww3.arb.ca.gov/ei/tools/pollution_map/doc/caveats%20document12_22_2017.pdf

[8] All but 39 facilities that emit local air pollution found in CARB's Pollution Mapping Tool have time-invariant GHG C&T regulatory status between 2008-2017. All 39 facilities with time-varying statuses switch status only in 2017. Because we do not know if these switches are due to actual changes in regulatory status or coding errors, we drop these 39 facilities from our sample. An unreported robustness check shows that our results are not affected when we include these 39 facilities and recode their 2017 regulatory status with their 2008-2016 regulatory status.

4 Empirical approach

Our analysis proceeds along three steps. First, we use facility-by-year-level data to predict NO_x, SO_x, $PM_{2.5}$, and PM_{10} emissions driven by California's GHG C&T program. Second, we feed predicted emissions into an atmospheric transport model to generate zip code-by-year-level exposure of these pollutants driven by the program. Third, we examine whether the GHG C&T program changed the exposure gap for these pollutants between disadvantaged and other communities following its 2013 introduction.

Step 1: Isolating facility emissions driven by C&T   We exploit the unique facility-level eligibility criteria and 2013 timing of the GHG C&T program to isolate C&T-driven annual NO_x, SO_x, $PM_{2.5}$, and PM_{10} facility-level emissions during 2008-2017. Let j index facilities required to report annual pollution emissions to CARB. $C_j \in \{0, 1\}$ is GHG C&T regulatory status with $C_j = 1$ indicating that facility j is regulated. For facility j in year t, Y_{jt}^p is annual emissions of local pollutant $p \in \{NO_x, SO_x, PM_{2.5}, PM_{10}\}$. To isolate differential emission trends driven by the GHG C&T program, we estimate the following specification:

$$\ln Y_{jt}^p = \kappa_1^p [C_j \times t] + \kappa_2^p [C_j \times \mathbf{1}(t \geq 2013) \times t] + \phi_j^p + \gamma_t^p + \mu_{jt}^p \tag{1}$$

where μ_{jt}^p is an error term. To facilitate an emission trends interpretation, we include facility-specific dummy variables ϕ_j^p to remove time-invariant determinants of pollution p for facility j. To further enable a comparison of emission trends between C&T regulated and non-regulated facilities, we include year-specific dummy variables γ_t^p to remove common determinants of pollution p affecting all sample facilities in year t, such as California-wide economic conditions.

After estimating equation (1), we construct facility-by-year emissions of pollutant p that is driven solely by the C&T program (relative to California-wide determinants of pollution), by applying an exponential transformation to $\widehat{\kappa}_1^p [C_j \times t] + \widehat{\kappa}_2^p [C_j \times \mathbf{1}(t \geq 2013) \times t] + \widehat{\phi}_j^p$, where the hat notation indicates estimated parameters. Because facilities vary by average emission levels within our sample period, the inclusion of facility-level fixed effects, $\widehat{\phi}_j^p$, allows us to generate heterogeneous C&T-driven abatement across regulated facilities despite estimating a common percentage effect across regulated firms.[9] Figure S1 shows this abatement heterogeneity, displaying the distribution of facility-level predicted abatement driven by the C&T policy between 2012-2017 for NO_x, SO_x, $PM_{2.5}$, and PM_{10}.[10]

---

[9]For example, a 10% abatement effect implies 10 tons of abatement for a facility with 100 tons of average annual emissions and 5 tons of abatement for a facility with 50 tons of average annual emissions.

[10]A potential concern about this method to isolate GHG C&T-driven emissions is the possibility of policies targeting these pollutants introduced as the same time as the GHG C&T program. To our knowledge, there

Step 2: Modeling pollution transport   We next determine how C&T-driven pollution emissions is spatially dispersed across California. The standard approach is for the researcher to prescribe the set of locations exposed to emissions from a particular source, either by assuming emissions only affect a particular administrative unit or locations within a particular distance of the source. For example, one may assume emissions from Los Angeles county only affect Los Angeles county or the set of counties within a certain radial distance of Los Angeles county. Actual pollution dispersal from Los Angeles, however, may not conform to these assumptions and instead may vary depending on meteorological conditions and topography. To fully capture the complexity of pollution transport, we turn to an atmospheric transport model.

We input predicted facility-by-year NO_x, SO_x, $PM_{2.5}$, and PM_{10} emissions from step 1, together with the location and stack height of each facility, into the Hybrid Single Particle Lagrangian Integrated Trajectory Model (HYSPLIT), an atmospheric transport model developed by the U.S. National Oceanographic and Atmospheric Administration (NOAA) with meteorological conditions from NOAA's 40-km resolution North American Model Data Assimilation System (NAMDAS) (Draxler and Hess, 1998).

We choose HYSPLIT because it provides a middle-of-the-road approach for our application, balancing atmospheric realism with computational tractability. For example, HYSPLIT is less computationally intensive than chemical transport models such as WRF-Chem, but at the cost of not being able to model secondary pollutants. At the same time, HYSPLIT is more reliable when modeling pollution transport beyond 50 kilometers, which less computationally-intensive Gaussian-plume models like AERMOD or APEEP do poorly (EPA, 2015).

We note several aspects of our HYSPLIT implementation. First, to account for meteorological conditions that vary hourly, for each C&T-driven facility-level annual emission, we run forward particle trajectories at 00:00, 06:00, 12:00, and 18:00 for every day of the year, implicitly assuming that annual emissions are distributed uniformly within the year. Each trajectory runs for 24 hours, a duration long enough to ensure most emitted particles leave California. Second, because HYSPLIT does not explicitly account for particle decay, we apply half-life parameters from the atmospheric chemistry literature set at 3.8 hours for NO_x (Liu et al., 2016), 13 hours for SO_x (Lee et al., 2011), and 24 hours for $PM_{2.5}$ and PM_{10}(U.S. EPA, 2018). Third, we assume that a particle no longer contributes to surface pollution concentrations once it exits the planetary boundary layer, beyond which there is far less turbulent mixing. We conservatively set the boundary layer height at 1 km above the surface, which is about double the typical height for California (Rahn and Mitchell,

---

was no local air pollution policy introduced in 2013.

2016). As an illustration of pollution dispersal modeled by HYSPLIT, Figure 1b shows the trajectories of pollution emitted by a regulated facility in Los Angeles during 2016. In total, we compute over 11 million particle trajectories from over 300 regulated facilities between 2008-2017.

Finally, to obtain zip code-by-year pollution exposure (in $\mu g/m^3$) due to GHG C&T-driven emissions, we sum across HYSPLIT trajectories for each zip code and year and divide by the volume of the atmosphere between a zip code's surface and the boundary layer. We further divide by 365 to obtain an average daily measure of HYSPLIT-generated pollution exposure. Figure 1c show our benchmark HYSPLIT-generated daily exposure (in $\mu g/m^3/day$) for each zip code, averaged across 2008-2017 for NO_x. Figure S2 similarly shows average 2008-2017 zip-code exposure for SO_x, $PM_{2.5}$, and PM_{10}.[11]

To examine whether HYSPLIT-generated air pollution exposure correlates with ambient air pollution, we match zip code-level HYSPLIT-generated pollution exposure averaged over 2008-2017 to the average ambient pollution of that zip code as recorded by pollution monitors averaged over the same period, obtained from the U.S. Environmental Protection Agency.[12] Note that a perfect model fit is not expected as ambient pollution at any location originates from many more sources (i.e., stationary and non-stationary, within and beyond California) than the subset of California stationary sources regulated by the state's GHG C&T program. However, a positive correlation between the two pollution exposure measures would provide reassurance that HYSPLIT-generated pollution exposure from C&T regulated facilities is being detected by ambient pollution monitors. The positive correlations shown in Table S2 indicate that is indeed the case.[13]

While HYSPLIT incorporates high-frequency atmospheric conditions to determine trajectories of C&T-driven facility-level emissions, there is one major limitation. HYSPLIT does not incorporate atmospheric chemistry and thus omits secondary pollution such as particulates. To see if secondary $PM_{2.5}$ exposure exhibits a different spatial pattern than primary $PM_{2.5}$ exposure, in a robustness check, we replace the use of HYSPLIT in step 2 with InMAP, a reduced-complexity transport model based on the WRF-Chem model which incorporates secondary pollutants (Tessum, Hill and Marshall, 2017).

---

[11]Figure 1, Figure S2, and Table S3 show that criteria air pollution from GHG C&T-regulated facilities disperses across all of California and not just zip codes designated as disadvantaged. This implies that any change in average pollution exposure between disadvantaged and other zip codes occurs because the GHG C&T program alters the differential exposure between disadvantaged and other zip codes.

[12]Available here: https://www.arcgis.com/home/item.html?id=8d2012a2016e484dafaac0451f9aea24

[13]We are interested in modeling where C&T-driven pollution goes. As such, we do not directly use ambient pollution data (either from ground-based monitoring stations or remotely-sensed satellites) in our analysis as it is often difficult to determine which component of any location's ambient pollution originates from C&T-regulated facilities. Such "backwards" atmospheric modeling often yield indeterminate results.

Part 3: Estimating the C&T driven change in the EJ gap Finally, we examine whether California's GHG C&T program changed the pollution exposure gap between disadvantaged and other communities, or the EJ gap. Let $D_i \in \{0, 1\}$ denote disadvantaged status, with $D_i = 1$ indicating that zip code i contains all or part of a "Disadvantaged Community Census Tract," as defined by Senate Bill 535. For zip code i in year t, we take HYSPLIT-generated C&T-driven pollution exposure, E_{it}^p for pollutant $p \in \{NO_x, SO_x, PM_{2.5}, PM_{10}\}$, and estimate the following specification:

$$E_{it}^p = \beta_1^p[D_i \times t] + \beta_2^p[D_i \times \mathbf{1}(t \geq 2013) \times t] + \psi_i^p + \delta_t^p + \epsilon_{it}^p \tag{2}$$

where ψ_i^p are zip code-specific dummies and δ_t^p are year-specific dummies. β_1^p captures the linear trend in the average pollution exposure difference (from facilities that would eventually be regulated by the C&T program) between disadvantaged and other zip codes, or the EJ gap, during 2008-2012, before the GHG C&T program was introduced. $\beta_1^p > 0$ ($\beta_1^p < 0$) would indicate that the EJ gap was widening (narrowing) prior to the C&T program. We call β_1^p the "pre-C&T EJ gap trend." $\beta_1^p + \beta_2^p > 0$ captures the EJ gap trend after the program is introduced in 2013-2017, or the "post-C&T EJ gap trend." $\beta_1^p + \beta_2^p > 0$ ($\beta_1^p + \beta_2^p < 0$) would indicate that the GHG C&T program is widening (narrowing) the EJ gap. β_2^p captures the change in the EJ gap trend after the program's introduction, or the "post-C&T EJ gap trend break." As an alternative model, we also estimate a more flexible variant of equation 2 using annual EJ gap coefficients which allows the EJ gap to differ each year. We also estimate a version of equation 2 using log pollution exposure as the outcome.

For the baseline model, the error term, ϵ_{it}, is clustered at the county level to allow for arbitrary forms of heteroskedasticity and serial correlation within a county. To estimate an average pollution exposure effect across individuals in California, we further weight each zip code-by-year observation in equation (2) by average zip code population during 2008-2012. We choose the 2008-2012 period to avoid potential concerns about migration induced by the C&T program.

5   Results

We begin by examining the baseline EJ gap in 2008, before the introduction of the GHG C&T program. Consistent with prior work documenting existing EJ gaps both in California (Cushing et al., 2018) and elsewhere (Bullard, 2000; Bowen, 2002; Ringquist, 2005; Mohai, Pellow and Roberts, 2009; Banzhaf, Ma and Timmins, 2019), Table S3 shows that disadvantaged communities experienced higher levels of NO_x, SO_x, $PM_{2.5}$, and PM_{10} exposure in

2008 than other communities on average due to local air pollution emissions from facilities that would eventually be regulated by the C&T program.

We now turn to our main result examining the evolution of the EJ gap after 2008, as shown in Figure 2. Across all four pollutants, the EJ gap widens during 2008-2012, the period leading up to the start of the C&T program, as evident by the positive pre-C&T EJ gap trend (i.e., β_1^p from equation (2)) and the more flexibly estimated annual EJ gap coefficients prior to 2013. However, we find that the post-C&T EJ gap trend is negative following the 2013 introduction of the C&T program (i.e., $\beta_1^p + \beta_2^p$ from equation (2)). This drop in the EJ gap is large: during 2012-2017, the EJ gap narrowed at a faster annual rate than its previous expansion during 2008-2012. Between 2012 to 2017, the program reduced California's EJ gap by 21%, 24%, 30%, and 30% for NO_x, SO_x, $PM_{2.5}$, and PM_{10}, respectively. The difference in EJ gap trends before and after the program's introduction, or post-C&T EJ gap trend break (i.e., β_2^p from equation (2)), is statistically significant for all four pollutants. Table 1 displays coefficients from equation (2) as well as from the more flexibly estimated year-specific EJ gap model.

Robustness checks We consider several robustness checks. Within step 1, we conduct three robustness checks. The closure of the San Onofre Nuclear Generating Station, a major power plant in southern California, also occurred in 2013. This event impacted California's electricity sector which may confound our estimates (Davis and Hausman, 2016). To avoid these effects, we additional construct a measure of C&T-driven pollution exposure using only emissions from regulated non-electricity facilities. We obtain a similar estimate for β_2^p (M2 of Figure 3 and col. 2 of Table S4). Equation (1) models changes in the emissions difference between C&T regulated and non-regulated facility as linear trends. We find a similar estimate for β_2^p when we allow for more flexible year-specific differences in equation (1) (M3 of Figure 3 and col. 3 of Table S4). Next, rather than subdivide annual C&T-driven emissions uniformly across 4-hour intervals within a year, we instead use the within-year distribution of emissions for electricity facilities with Continuous Emissions Monitoring data, available from the U.S. EPA for NO_x and SO_x emissions. Imposing the within-year emissions distribution does not affect our EJ gap results for NO_x and SO_x (M4 of Figure 3 and col. 4 of Table S4).

We conduct four robustness checks within step 2. We use pollution half-life parameters taken from the atmospheric chemistry literature because HYSPLIT does not model pollution decay over time. Our estimate for β_2^p is relatively stable to whether we allow for a 10% larger half-life parameter which implies a slower decay rate (M5 of Figure 3 and col. 2 Table S5) or a 10% smaller half-life parameter which implies a faster decay rate (M6 of Figure 3 and col.

3 of Table S5). Likewise our results are little affected if we lower the height of the planetary boundary layer to 0.5 km (M7 of Figure 3 and col. 4 Table S5) or raise it to 2 km (M8 of Figure 3 and col. 5 Table S5).

We conduct three robustness checks within step 3. The first set of checks consider alternative error structures. We find that our β_2^p becomes more precise when we allow errors to be spatially correlated within a uniform kernel across a distance of 500 km distance (Conley, 1999), roughly the longitudinal width of California, and serially correlated across 5 years (Newey and West, 1987) (M9 of Figure 3 and col. 6 of Table S5). Likewise, β_2^p becomes more precise when we allow for error terms to be correlated across the four local pollutants using a Seemingly Unrelated Regression (SUR) procedure (M10 of Figure 3 and col. 7 of Table S5). Equation (2) examines the EJ gap in daily pollution levels of $\mu g/m^3/day$, the unit of exposure typically used for air pollution policy and by the public health literature. In Table S6, we detect a statistically significant post-C&T EJ gap trend break when modeling pollution exposure in logs, showing that following 2013, C&T-driven exposure in disadvantaged communities decreased as a percentage of exposure in other communities.

Finally, to examine the potential role of secondary $PM_{2.5}$, we replace HYSPLIT in step 2 of our procedure with InMAP, a reduced-complexity transport model based on output from WRF-Chem, which models total (i.e., primary and secondary) $PM_{2.5}$ exposure from C&T-driven facility-level NO_x, SO_x, and $PM_{2.5}$ emissions (Tessum, Hill and Marshall, 2017).[14] InMAP, however, has one major limitation: it only employs transport patterns in 2005 whereas our sample period is 2008-2017. Because InMAP does not model transport patterns during our sample period, we are unable to directly compare estimates using InMAP-generated exposure with that using HYSPLIT-generated exposure.[15] Instead, we examine the role of secondary $PM_{2.5}$ by comparing how estimates of the EJ gap differ between InMAP-generated primary $PM_{2.5}$ exposure and InMAP-generated total $PM_{2.5}$ exposure. Table S8 replicates the structure of Table 1. Column 1 examines InMAP-generated primary $PM_{2.5}$ exposure while column 2 examines InMAP-generated total $PM_{2.5}$ exposure. Changes in the EJ gap are very similar for primary and total $PM_{2.5}$ exposure generated by InMap. This suggests that the EJ effect on primary pollution exposure may not be very different from that on total pollution exposure.

---

[14] In addition to the inputs used in HYSPLIT, InMap requires the diameter, temperature, and emissions velocity for each smokestack. We obtained these data from CARB. In the case of facilities with more than one stack, we use the mean value across stacks. In the case of the facilities with missing observations, we impute data using the industry-level average.

[15] Furthermore, there is a difference in units between HYSPLIT and InMap. For any given location, HYSPLIT produces the stock of pollution exposure during a given period, whereas InMAP produces that period's average flow of pollution exposure.

The importance of modeling pollution transport Our empirical approach explicitly embeds a pollution transport model within a causal inference framework. To examine the importance of modeling pollution transport for our results, we compare our approach with prevailing methods for assigning pollution exposure from emission sources. Specifically, we re-estimated the EJ effect under different commonly employed assumptions about how emissions disperse spatially. We fail to detect a statistically significant post-C&T EJ gap trend break (i.e., β_2^p in equation (2)) when we assume that pollution exposure from a facility is limited to the zip code of that facility (M1 of Fig. 4 and col. 1 of Table S7) and to zip codes with centroids that are within 1.6 km and 4 km distance circles around the facility (M2-3 of Fig. 4 and cols. 2-3 of Table S7). Attenuation of the EJ effect likely occurs because pollution typically disperses beyond the areas prescribed by these methods. The resulting pollution spillover leads to a violation of the Stable Unit Treatment Value Assumption (SUTVA) (see discussion in Deschenes and Meng (2018)).

More recent work use atmospheric transport models in a limited manner (Ash and Fetter, 2004; Morello-Frosch and Jesdale, 2006; Grainger and Ruangmas, 2018; Mansur and Sheriff, 2019). To reduce computational demands, these papers consider only "prevailing winds" by modeling one year of pollution transport, typically at the start of the sample period, and then imposing that transport pattern onto the rest of the sample period. To replicate this approach, we impose HYSPLIT trajectories from only 2008, only 2013, or only 2017 onto the rest of our sample years. We detect a negative effect for β_2^p. However, the magnitudes for β_2^p using this approach is 20-50% smaller than our benchmark estimates that fully model pollution transport every 4 hours throughout the 2008-2017 period (M4-6 of Fig. 4 and cols. 4-6 of Table S7).

6 Discussion

Many market settings are characterized by stark efficiency-equity trade-offs (Okun, 2015). We find that California's carbon market led to environmental justice co-benefits by dramatically narrowing the pollution exposure gap between disadvantaged and other communities. This result brings causal evidence to a long-standing debate that continues to shape one of the world's most ambitious climate policies. Moreover, the integration of pollution transport modeling and causal inference developed in this paper is broadly applicable across many questions that involve environmental valuation.

This paper has limitations that future studies can explore, both for California's cap-and-trade program and in other contexts. First, as with prior EJ studies, our analysis omits uncertainty arising from how pollution transport is modeled. One possibility involves resam-

pling meteorological conditions via a bootstrapping algorithm. Unfortunately, substantial computational advances must be made for this to be feasible: in our setting, one iteration of our three-step procedure currently takes about 10 hours on a high-performance computing cluster. Second, pollution exposure constitutes only one component of the many distributional consequences of California's cap-and-trade program. Questions remain regarding how the program alters the distribution of health outcomes as well as the cost burden of climate policy. Additionally, to fully understand welfare consequences, one must also account for sorting as households move in response to changes in the pollution exposure gap (Banzhaf, Ma and Timmins, 2019).

More generally, environmental markets may not always reduce the pollution exposure gap between disadvantaged and other communities, as it has in California. In settings where disadvantaged communities are downwind of high marginal abatement cost polluters, an environmental market could increase the environmental justice gap. Future research should theoretically characterize the general conditions under which environmental markets worsen or improve the environmental justice gap.

Exhibits

Figure 1: Modeling air pollution exposure driven by the cap-and-trade program
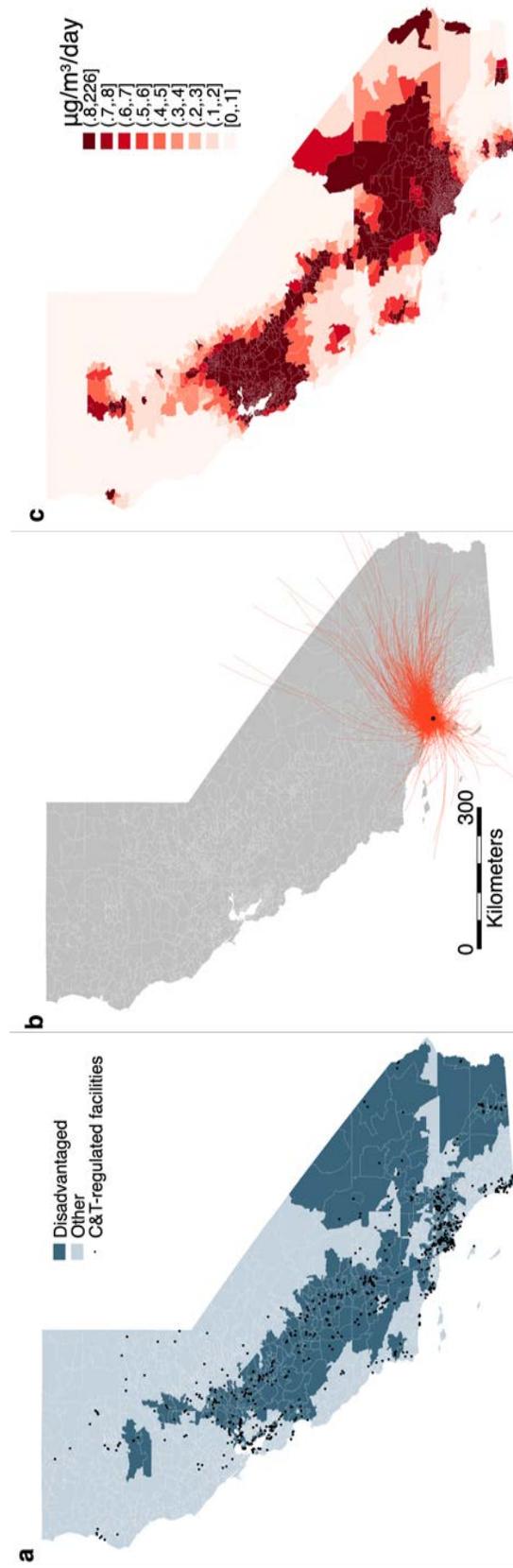
Figure illustrates how facility-level pollution emissions is converted to average daily zip code-level pollution exposure using a pollution transport model. Shading in panel (a) shows California zip codes that are legally designated as disadvantaged (dark blue) and zip codes that are not (light blue). Black dots show all stationary facilities regulated by California's GHG C&T program. Panel (b) shows HYSPLIT-generated particle trajectories every 4-hours from a polluting facility in Los Angeles during 2016. Panel (c) shows zip code-level average daily NO_x exposure (in $\mu g/m^3/day$) during 2008-2017 driven by facilities regulated by California's GHG C&T program as generated by HYSPLIT.

Figure 2: Environmental justice gap before and after the cap-and-trade program
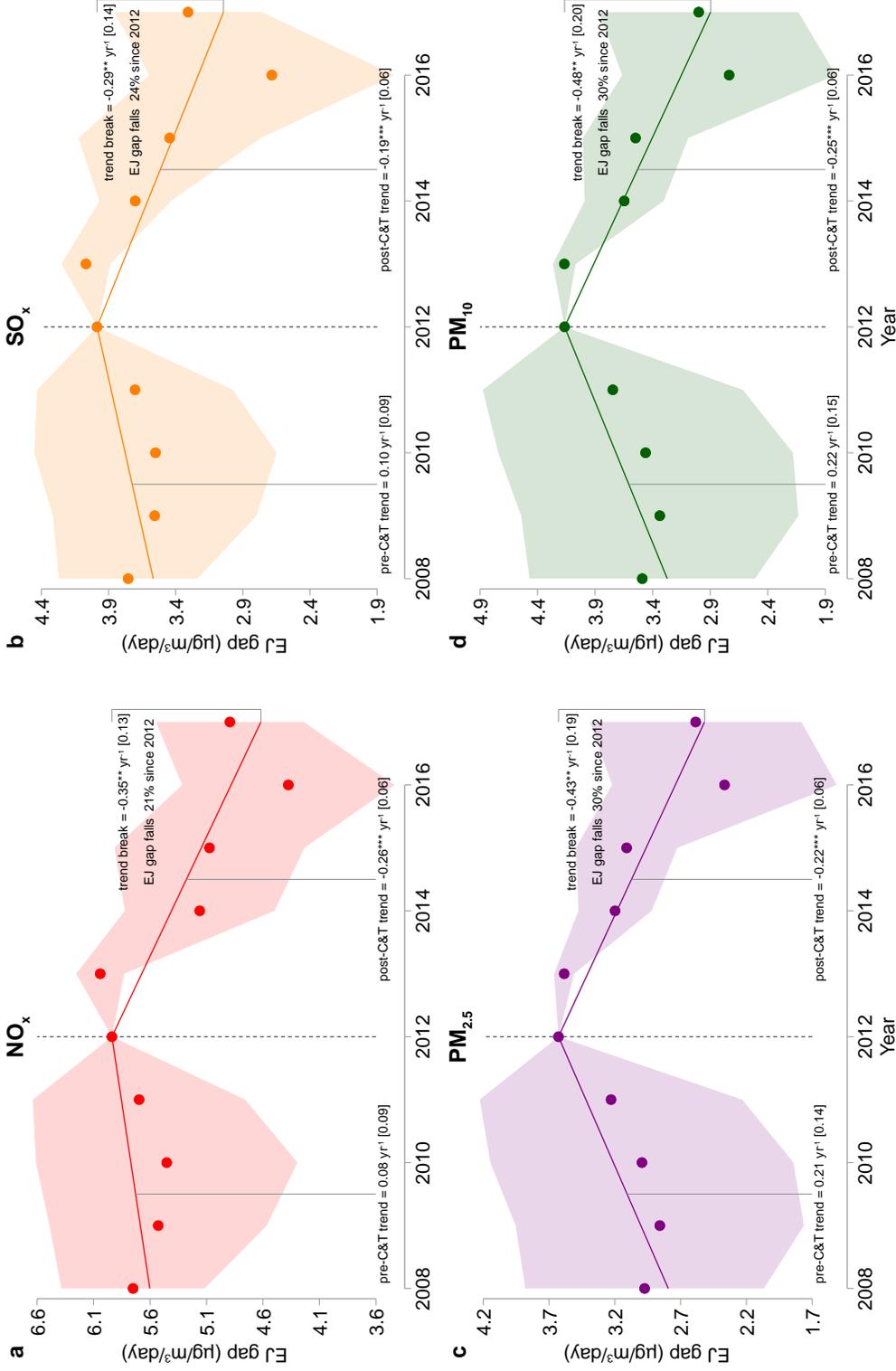
Panels (a)-(d) show the estimated average daily pollution exposure gap (in $\mu g/m^3/\text{day}$) between disadvantaged and other zip codes (i.e., "EJ gap") during 2008-2017 for NO_x, SO_x, $PM_{2.5}$, and PM_{10}, respectively. Dots show year-specific EJ gap with 95% confidence intervals. Solid lines show linear fit for EJ gap trend before (2008-2012) and after (2013-2017) the C&T program. Associated text indicates point estimates and standard errors for the pre-C&T linear trend coefficient, post-C&T linear trend coefficient, and the post-C&T trend break coefficient (i.e., β_1^p, $\beta_1^p + \beta_2^p$, and β_2^p in equation (2)). Percentage change in EJ gap calculated between 2012 and 2017. Standard errors in brackets clustered at the county-level. P-values from two-sided t-tests with *** p<0.01, ** p<0.05, * p<0.1. Estimates also reported in Table 1.

16

Figure 3: Robustness checks
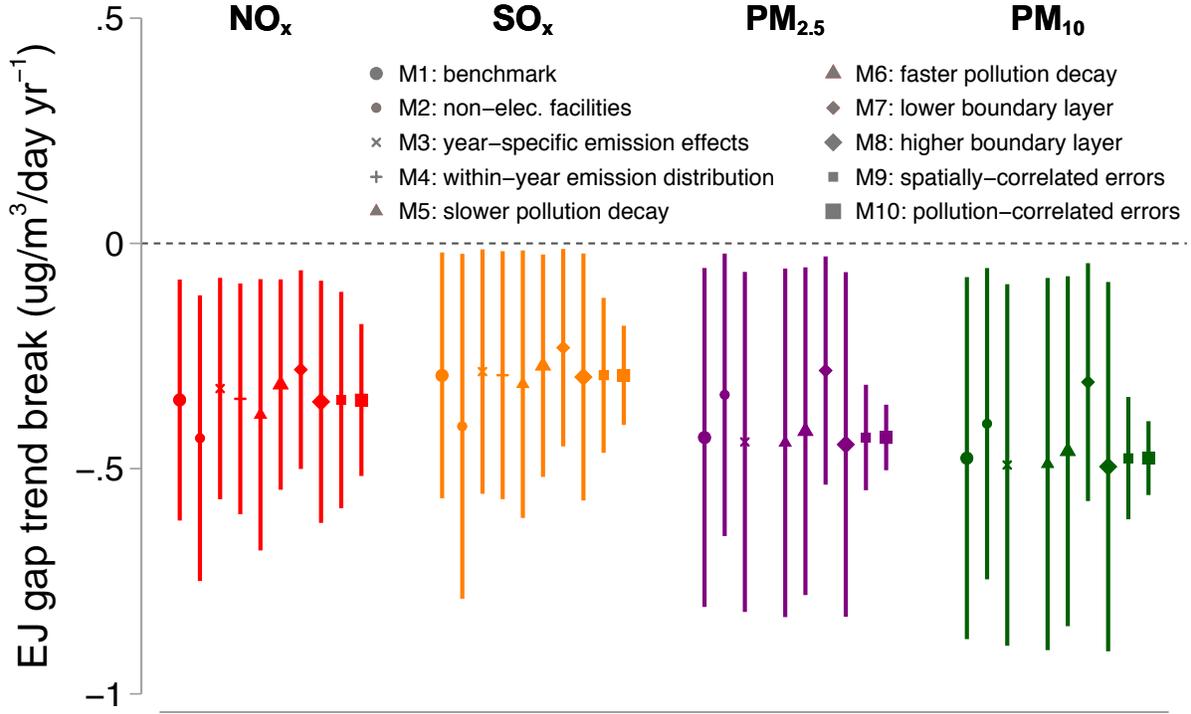
Point estimates and 95% confidence intervals of the change in the EJ gap trend (in avg. daily $\mu g/m^3 yr^{-1}$) after the introduction of the C&T program in 2013 (i.e., EJ gap trend break or β_2^p from equation (2)), for NO_x, SO_x, $PM_{2.5}$, and PM_{10} across robustness checks. M1: benchmark model. M2: using only non-electricity facilities to estimate C&T-driven emissions. M3: using year-specific effects to estimate C&T-driven emissions. M4: using the within-year distribution of emissions for electricity facilities (available for NO_x and SO_x only). M5: applying a slower pollution decay (i.e., 10% larger half-life parameter). M6: applying a faster pollution decay (i.e., 10% smaller half-life parameter). M7: applying a planetary boundary layer set at 0.5 km. M8: applying planetary boundary layer set at 2 km. M9: using standard errors adjusted for spatial (500 km uniform kernel) and serial correlation (5 years). M10: using standard errors that allow correlation across pollutants using a Seemingly Unrelated Regression (SUR) procedure. Estimates also reported in Tables S4-S5.

17

Figure 4: Importance of modeling pollution transport
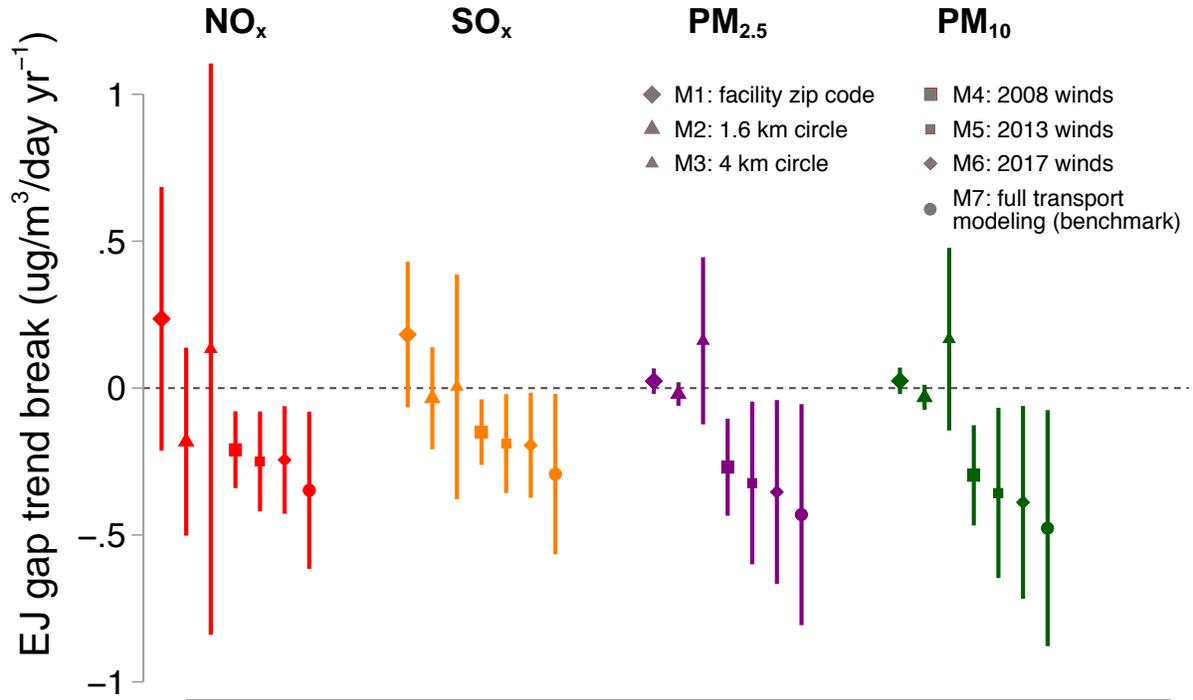
Point estimates and 95% confidence intervals of the change in the EJ gap trend (in avg. daily $\mu g/m^3yr^{-1}$) after the introduction of the C&T program in 2013 (i.e., EJ gap trend break or β_2^p from equation (2)), for NO_x, SO_x, $PM_{2.5}$, and PM_{10} across different approaches for assigning pollution exposure from sources. M1: pollution exposure assigned only to zip code of emitting facility. M2-3: pollution exposure assigned to zip codes with centroid within 1.6 km and 4 km circle of emitting facility, respectively. M4-6: pollution exposure based on transport pattern only in 2008, 2013, and 2017, respectively. M7: benchmark pollution exposure with pollution transport modeled every 4 hours throughout 2008-2017. Estimates also reported in Table S7.

Table 1: Environmental justice gap before and after cap-and-trade

	(1) NO_x	(2) SO_x	(3) $PM_{2.5}$	(4) PM_{10}
	Panel a: Trend-break model			
EJ gap:				
pre-C&T trend (β_1^p)	0.08	0.10	0.21	0.22
	[0.09]	[0.09]	[0.14]	[0.15]
post-C&T trend ($\beta_1^p + \beta_2^p$)	-0.26***	-0.19***	-0.22***	-0.25***
	[0.06]	[0.06]	[0.06]	[0.06]
post-C&T trend break (β_2^p)	-0.35**	-0.29**	-0.43**	-0.48**
	[0.13]	[0.14]	[0.19]	[0.20]
EJ gap pct. change since 2012	21%	24%	30%	30%
	Panel b: Year-specific effects model			
EJ gap:				
in 2008	-0.19	-0.23	-0.65	-0.67
	[0.32]	[0.26]	[0.45]	[0.49]
in 2009	-0.41	-0.43	-0.77	-0.83
	[0.48]	[0.38]	[0.55]	[0.60]
in 2010	-0.49	-0.44	-0.63	-0.70
	[0.58]	[0.45]	[0.58]	[0.64]
in 2011	-0.24	-0.28	-0.40	-0.42
	[0.47]	[0.36]	[0.50]	[0.56]
in 2012	-	-	-	-
in 2013	0.10	0.08	-0.04	0.00
	[0.11]	[0.09]	[0.04]	[0.05]
in 2014	-0.78**	-0.28**	-0.43***	-0.52***
	[0.33]	[0.13]	[0.14]	[0.17]
in 2015	-0.86**	-0.54	-0.52***	-0.62***
	[0.42]	[0.34]	[0.19]	[0.23]
in 2016	-1.56***	-1.30***	-1.26***	-1.43***
	[0.47]	[0.46]	[0.43]	[0.46]
in 2017	-1.04***	-0.68**	-1.04**	-1.16***
	[0.33]	[0.27]	[0.40]	[0.43]
Zip codes	1650	1650	1650	1650
Observations	16,488	16,488	16,488	16,488

NOTES: Panel (a) shows estimates of the pre-C&T EJ gap trend (i.e., β_1^p from equation (2)), post-C&T EJ gap trend (i.e., $\beta_1^p + \beta_2^p$ from equation (2)), and and post-C&T EJ gap trend break (i.e., β_2^p from equation (2)) for NO_x, SO_x, $PM_{2.5}$, and PM_{10}, across columns. Percentage change in EJ gap calculated between 2012 and 2017. Panel (b) shows a more flexible version of equation (2) by estimating year-specific EJ gaps with 2012 being the omitted year. All models include zip code-specific and year-specific dummy variables. Observations weighted by zip code-level average population during 2008-2012. Standard errors clustered at the county-level in brackets. P-values from two-sided t-tests with *** p<0.01, ** p<0.05, * p<0.1.

References

Ash, Michael, and T. Robert Fetter. 2004. "Who Lives on the Wrong Side of the Environmental Tracks? Evidence from the EPA's Risk-Screening Environmental Indicators Model." *Social Science Quarterly*, 85(2): 441–462.

Banzhaf, Spencer, Lala Ma, and Christopher Timmins. 2019. "Environmental Justice: The Economics of Race, Place, and Pollution." *Journal of Economic Perspectives*, 33(1): 185–208.

Bowen, William. 2002. "An Analytical Review of Environmental Justice Research: What do we Really Know?" *Environmental Management*, 29(1): 3–15.

Bullard, Robert. 2000. *Dumping in Dixie: Race, Class, and Environmental Quality.* Westview Press.

Burtraw, Dallas, David A Evans, Alan Krupnick, Karen Palmer, and Russell Toth. 2005. "Economics of Pollution Trading for SO2 and NO x." *Annu. Rev. Environ. Resour.*, 30: 253–289.

Chinn, Lily N. 1999. "Can the Market Be Fair and Efficient? An Environmental Justice Critique of Emissions Trading." *Ecology Law Quarterly*, 26(1): 80–125.

Conley, Timothy G. 1999. "GMM Estimation with Cross Sectional Dependence." *Journal of Econometrics*, 92(1): 1–45.

Corburn, Jason. 2001. "Emissions Trading and Environmental Justice: Distributive Fairness and the USA's Acid Rain Programme." *Environmental Conservation*, 28(4): 323–332.

Costello, Christopher, Daniel Ovando, Tyler Clavelle, C. Kent Strauss, Ray Hilborn, Michael C. Melnychuk, Trevor A. Branch, Steven D. Gaines, Cody S. Szuwalski, Reniel B. Cabral, Douglas N. Rader, and Amanda Leland. 2016. "Global Fishery Prospects under Contrasting Management Regimes." *Proceedings of the National Academy of Sciences*, 113(18): 5125–5129.

Cushing, Lara, Dan Blaustein-Rejto, Madeline Wander, Manuel Pastor, James Sadd, Allen Zhu, and Rachel Morello-Frosch. 2018. "Carbon Trading, Co-pollutants, and Environmental Equity: Evidence from California's cap-and-trade program (2011–2015)." *PLoS medicine*, 15(7): e1002604.

Dales, John H. 1968. *Pollution, Property and Prices: An Essay in Policy.* Toronto: University of Toronto Press.

Davis, Lucas, and Catherine Hausman. 2016. "Market Impacts of a Nuclear Power Plant Closure." *American Economic Journal: Applied Economics*, 8(2): 92–122.

Deschenes, Olivier, and Kyle C Meng. 2018. "Quasi-experimental Methods in Environmental Economics: Challenges and Opportunities." *Handbook of Environmental Economics*, 4: 285.

Draxler, Roland R, and GD Hess. 1998. "An Overview of the $HYSPLIT_4$ Modelling System for Trajectories." *Australian Meteorological Magazine*, 47(4): 295–308.

EPA, US. 2015. "Revision to the Guideline on Air Quality Models: Enhancements to the AERMOD Dispersion Modeling System and Incorporation of Approaches to Address Ozone and Fine Particulate Matter." US Environmental Protection Agency Working Paper 2060-AS54.

Fowlie, Meredith, Stephen P. Holland, and Erin T. Mansur. 2012. "What Do Emissions Markets Deliver and to Whom? Evidence from Southern California's NO_x Trading Program." *American Economic Review*, 102(2): 965–93.

Graff Zivin, Joshua, and Matthew Neidell. 2013. "Environment, health, and human capital." *Journal of Economic Literature*, 51(3): 689–730.

Grainger, Corbett, and Thanicha Ruangmas. 2018. "Who Wins from Emissions Trading? Evidence from California." *Environmental and Resource Economics*, 71(3): 703–727.

Greenstone, Michael, and Ted Gayer. 2009. "Quasi-experimental and Experimental Approaches to Environmental Economics." *Journal of Environmental Economics and Management*, 57(1): 21 – 44. Frontiers of Environmental and Resource Economics.

Herron, Elise. 2019. "Oregon Clean Energy Jobs Bill Has Mixed Support From Environmental Justice Groups." *Willamette Week*.

Leber, Rebecca. 2016. "The most Dramatic Climate Fight of the Election is in Washington State." *Grist*.

Lee, Chulkyu, Randall V Martin, Aaron van Donkelaar, Hanlim Lee, Russell R Dickerson, Jennifer C Hains, Nickolay Krotkov, Andreas Richter, Konstantine Vinnikov, and James J Schwab. 2011. "SO_2 Emissions and Lifetimes: Estimates from Inverse Modeling using in situ and global, space-based (SCIAMACHY and OMI) Observations." *Journal of Geophysical Research: Atmospheres*, 116(D6).

Liu, Fei, Steffen Beirle, Qiang Zhang, Steffen Dörner, Kebin He, and Thomas Wagner. 2016. "NO$_x$ Lifetimes and Emissions of Cities and Power Plants in Polluted Background Estimated by Satellite Observations." *Atmospheric Chemistry and Physics*, 16(8): 5283–5298.

Mansur, Erin T., and Glenn Sheriff. 2019. "Do Pollution Markets Harm Low Income and Minority Communities? Ranking Emissions Distributions Generated by California's RE-CLAIM Program." National Bureau of Economic Research Working Paper 25666.

Megerian, Chris. 2017. "In the battle over California Climate Policies, Green Projects are now in the Hot Seat." *Los Angeles Times*.

Meng, Kyle C. 2019. "Is Cap-and-Trade Causing More Greenhouse Gas Emissions in Disadvantaged Communities?" PERC PERC Policy Report.

Mohai, Paul, David Pellow, and J. Timmons Roberts. 2009. "Environmental Justice." *Annual Review of Environment and Resources*, 34(1): 405–430.

Montgomery, W. David. 1972. "Markets in Licenses and Efficient Pollution Control Programs." *Journal of Economic Theory*, 5(3): 395 – 418.

Morello-Frosch, Rachel, and Bill M Jesdale. 2006. "Separate and Unequal: Residential Segregation and Estimated Cancer Risks Associated with Ambient Air Toxics in US Metropolitan Areas." *Environmental Health Perspectives*, 114(3): 386.

Newey, Whitney K., and Kenneth D. West. 1987. "A Simple, Positive Semi-Definite, Heteroskedasticity and Autocorrelation Consistent Covariance Matrix." *Econometrica*, 55(3): 703–708.

Okun, Arthur M. 2015. *Equality and Efficiency: The Big Tradeoff.* Brookings Institution Press.

Rahn, David A., and Christopher J. Mitchell. 2016. "Diurnal Climatology of the Boundary Layer in Southern California Using AMDAR Temperature and Wind Profiles." *Journal of Applied Meteorology and Climatology*, 55(5): 1123–1137.

Ringquist, Evan J. 2005. "Assessing Evidence of Environmental Inequities: A Meta-analysis." *Journal of Policy Analysis and Management*, 24(2): 223–247.

Ringquist, Evan J. 2011. "Trading Equity for Efficiency in Environmental Protection? Environmental Justice Effects from the SO$_2$ Allowance Trading Program." *Social Science Quarterly*, 92(2): 297–323.

Salzman, James, Genevieve Bennett, Nathaniel Carroll, Allie Goldstein, and Michael Jenkins. 2018. "The Global Status and Trends of Payments for Ecosystem Services." *Nature Sustainability*, 1(3): 136–144.

Takade, Penni. 2013. "Association of Irritated Residents v. California Air Resources Board: Climate Change and Environmental Justice." *Ecology Law Quarterly*, 40: 573.

Tessum, Christopher W., Jason D. Hill, and Julian D. Marshall. 2017. "InMAP: A model for air pollution interventions." *PLOS ONE*, 12(4): 1–26.

Transnational Institute. 2013. "It is Time to Scrap the ETS! ."

U.S. EPA. 2018. "User's Guide for the AMS/EPA Regulatory Model AERMOD."

Walch, Ryan. 2019. "The Effect of California's Carbon Cap and Trade Program on Co-pollutants and Environmental Justice: Evidence from the Electricity Sector." *mimeo*.

World Bank Group. 2019. "State and Trends of Carbon Pricing."

Supplementary Figures

Figure S1: Facility-level C&T-driven abatement between 2012-2017
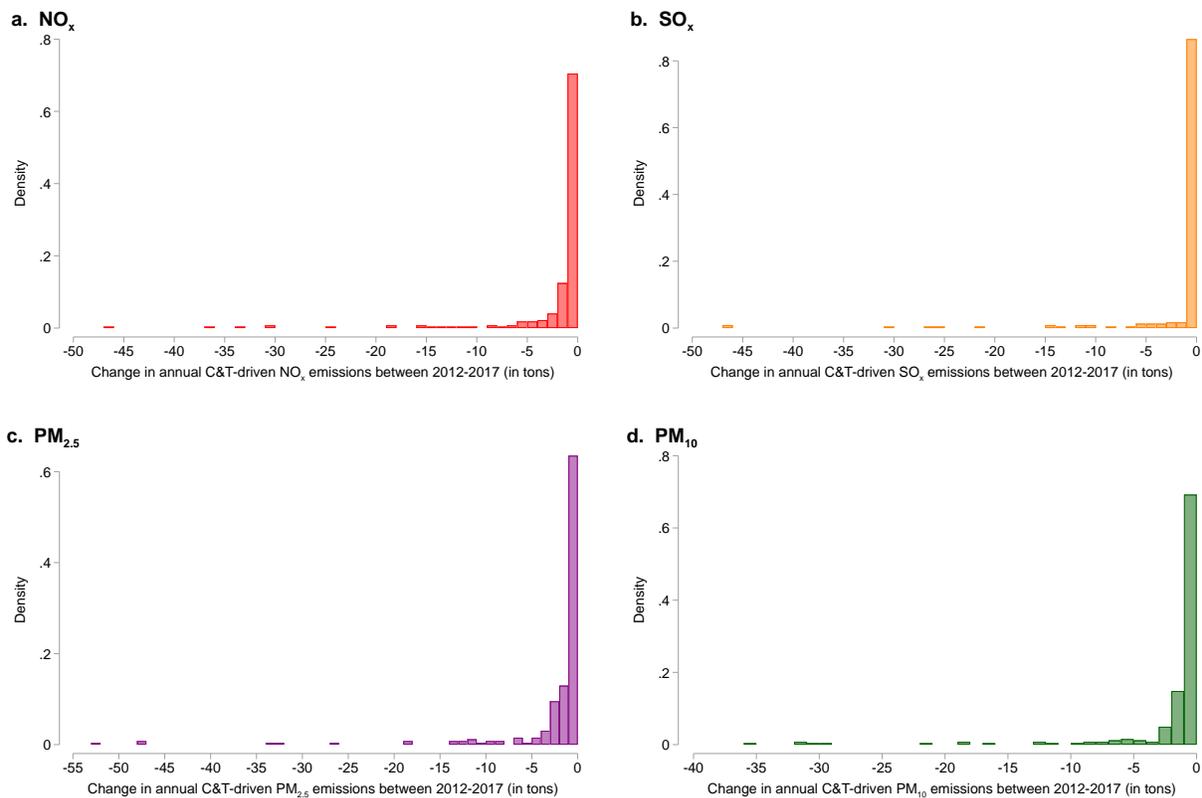
Panels (a)-(d) show the distribution of facility-level change in C&T-driven pollution abatement between 2012-2017 predicted from step 1 for NO_x, SO_x, $PM_{2.5}$, and PM_{10}, respectively.

Figure S2: Average pollution exposure driven by C&T regulated facilities
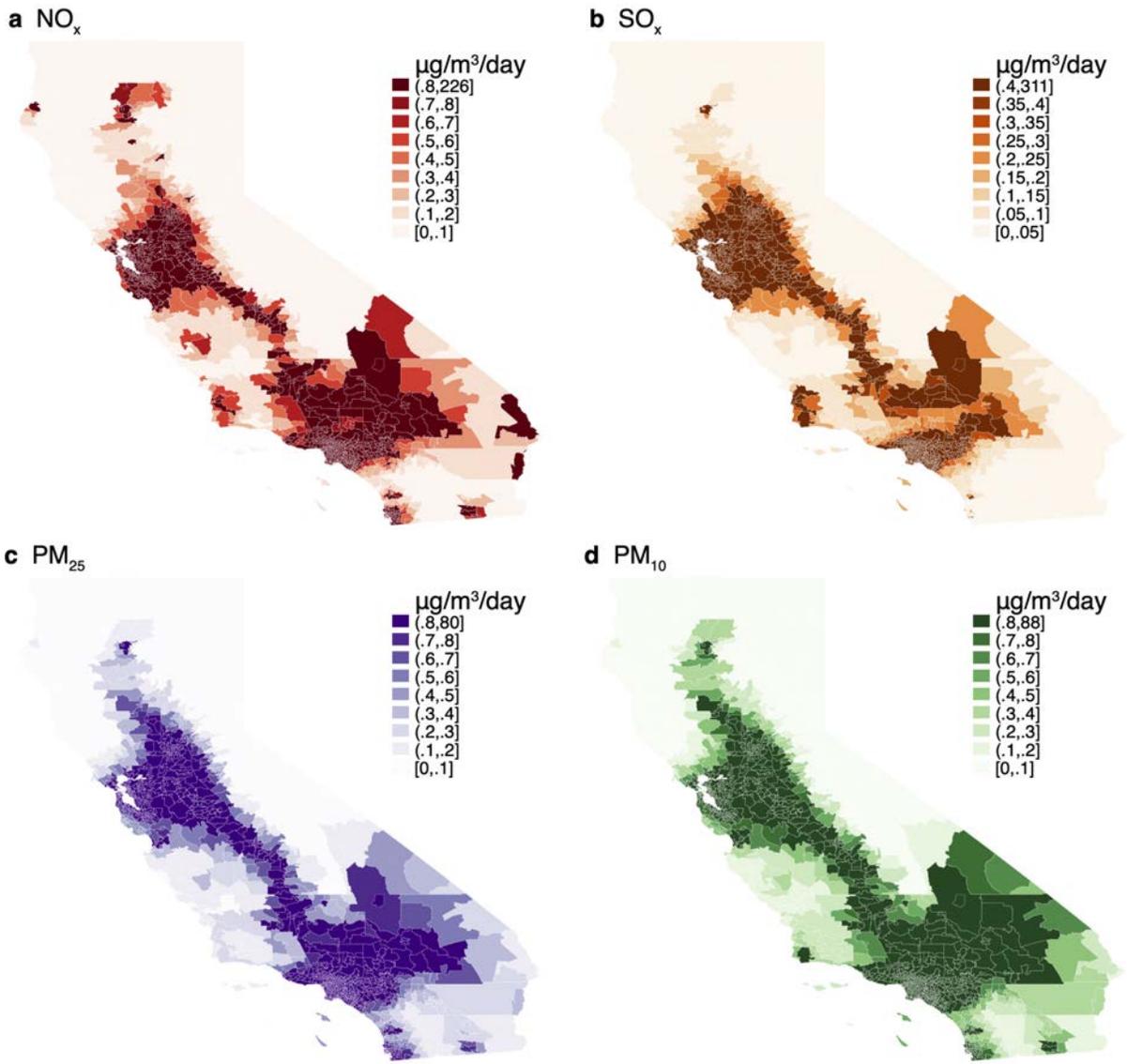
Panels (a)-(d) show daily exposure (in $\mu g/m^3/day$) for each zip code averaged across 2008-2017 from GHG C&T-regulated facilities as modeled in step 2 generated by HYSPLIT for NO_x, SO_x, $PM_{2.5}$, and PM_{10}, respectively.

Supplementary Tables

Table S1: GHG cap-and-trade regulated and non-regulated facilities

	C&T regulated facilities	non-C&T regulated facilities
All	306	440
By sector:		
Cement	9	2
Cogeneration	52	7
Electricity	70	173
Hydrogen	7	0
Oil	46	41
Other	102	213
Refinery	20	4

NOTES: Total number of sample GHG cap-and-trade regulated and non-regulated facilities and by sector.

Table S2: Correlation between HYSPLIT-driven and ambient pollution exposure

	(1)	(2)	(3)	(4)
	Outcome is ambient ln exposure			
	ln NO_x	ln SO_x	ln $PM_{2.5}$	ln PM_{10}
HYSPLIT-driven ln exposure	0.16***	0.09	0.09***	0.09***
	[0.03]	[0.07]	[0.03]	[0.02]
Zip codes	95	32	86	94

NOTES: Linear coefficient from zip code-level regressions of ln daily HYSPLIT-driven pollution exposure (in $\mu g/m^3/day$) averaged across 2008-2017 on ln daily pollution exposure from ambient pollution monitors (in $\mu g/m^3/day$) averaged across 2008-2017. We employ a ln-ln specification because ambient pollution readings, which capture the average daily instantaneous stock of pollution, are not directly comparable to our exposure measure, which capture average daily pollution flow from C&T-driven emissions. Ambient pollution are assumed to be uniformly distributed within a monitor's zip code. To reduce measurement error from zip codes with large areas, we restrict the sample of California zip codes with ambient monitors to zip codes with area below the mean. Standard errors clustered at the county-level in brackets. P-values from two-sided t-tests with *** p<0.01, ** p<0.05, * p<0.1.

Table S3: Pollution exposure difference between disadvantaged and other zip codes in 2008

	(1) Disadvantaged	(2) Other	(3) Difference
NO_x	8.14	2.35	5.80***
	(19.49)	(7.93)	[0.77]
SO_x	5.06	1.28	3.79***
	(16.57)	(3.89)	[0.63]
$PM_{2.5}$	4.22	1.24	2.98***
	(5.91)	(3.09)	[0.24]
PM_{10}	4.94	1.44	3.50***
	(6.67)	(3.42)	[0.27]
Zip codes	722	990	1,712

NOTES: Column 1 shows average 2008 pollution exposure ($\mu g/m^3$) across disadvantaged zip codes, with standard deviation in parentheses. Column 2 shows average 2008 pollution exposure ($\mu g/m^3$) across other zip codes, with standard deviation in parentheses. Column 3 shows the average difference in 2008 pollution exposure between disadvantaged and other zip codes, with standard error in brackets. All pollution exposure generated by HYSPLIT from facilities that would eventually be regulated by the GHG C&T program. P-values from two-sided t-tests with *** $p<0.01$, ** $p<0.05$, * $p<0.1$.

Table S4: Robustness: Step 1

	(1)	(2)	(3)	(4)
	Benchmark	Non elec. facilities	Year-specific effects	Within-year emissions dist.

		Panel a: NO$_x$		
EJ gap:				
pre-C&T trend (β_1^p)	0.08	0.21	0.06	0.07
	[0.09]	[0.13]	[0.08]	[0.08]
post-C&T trend break (β_2^p)	-0.35**	-0.43***	-0.32**	-0.35***
	[0.13]	[0.16]	[0.12]	[0.13]
Observations	16,488	16,444	16,491	16,488

		Panel b: SO$_x$		
EJ gap:				
pre-C&T trend (β_1^p)	0.10	0.16	0.10	0.10
	[0.09]	[0.11]	[0.09]	[0.08]
post-C&T trend break (β_2^p)	-0.29**	-0.41**	-0.28**	-0.29**
	[0.14]	[0.19]	[0.14]	[0.14]
Observations	16,488	16,444	16,491	16,488

		Panel c: PM$_{2.5}$		
EJ gap:				
pre-C&T trend (β_1^p)	0.21	0.18	0.22	0.21
	[0.14]	[0.13]	[0.14]	[0.14]
post-C&T trend break (β_2^p)	-0.43**	-0.34**	-0.44**	-0.43**
	[0.19]	[0.16]	[0.19]	[0.19]
Observations	16,488	16,444	16,491	16,488

		Panel d: PM$_{10}$		
EJ gap:				
pre-C&T trend (β_1^p)	0.22	0.26*	0.23	0.22
	[0.15]	[0.15]	[0.15]	[0.15]
post-C&T trend break (β_2^p)	-0.48**	-0.40**	-0.49**	-0.48**
	[0.20]	[0.17]	[0.20]	[0.20]
Observations	16,488	16,444	16,491	16,488

NOTES: Estimates of the pre-C&T EJ gap trend (i.e., β_1^p from equation (2)) and post-C&T EJ gap trend break (i.e., β_2^p from equation (2)) for NO$_x$, SO$_x$, PM$_{2.5}$, and PM$_{10}$ down panels. All models include zip code-specific and year-specific dummy variables. Observations weighted by zip code-level average population during 2008-2012. Column 1 shows the benchmark model. Column 2 uses only non-electricity facilities to estimate C&T-driven emissions. Column 3 uses year-specific effects to estimate C&T-driven emissions. Column 4 uses the within-year distribution of emissions for electricity facilities (available for NO$_x$ and SO$_x$ only). Standard errors clustered at the county-level in brackets. P-values from two-sided t-tests with *** p<0.01, ** p<0.05, * p<0.1.

Table S5: Robustness: Steps 2 and 3

	(1) Benchmark	(2) Slower decay	(3) Faster decay	(4) Lower boundary	(5) Higher boundary	(6) Spatial corr. err.	(7) Pollution corr. err.
Panel a: NO_x							
EJ gap:							
pre-C&T trend (β_1^p)	0.08	0.10	0.07	0.04	0.09	0.08	0.08
	[0.09]	[0.10]	[0.08]	[0.08]	[0.09]	[0.07]	[0.05]
post-C&T trend break (β_2^p)	-0.35**	-0.38**	-0.31***	-0.28**	-0.35**	-0.35***	-0.35***
	[0.13]	[0.15]	[0.12]	[0.11]	[0.13]	[0.12]	[0.09]
Observations	16,488	16,488	16,488	16,470	16,491	16,488	16,488
Panel b: SO_x							
EJ gap:							
pre-C&T trend (β_1^p)	0.10	0.12	0.09	0.07	0.11	0.10**	0.10***
	[0.09]	[0.09]	[0.08]	[0.07]	[0.09]	[0.04]	[0.04]
post-C&T trend break (β_2^p)	-0.29**	-0.31**	-0.27**	-0.23**	-0.30**	-0.29***	-0.29***
	[0.14]	[0.15]	[0.12]	[0.11]	[0.14]	[0.09]	[0.06]
Observations	16,488	16,488	16,488	16,470	16,491	16,488	16,488
Panel c: $PM_{2.5}$							
EJ gap:							
pre-C&T trend (β_1^p)	0.21	0.22	0.20	0.12	0.22	0.21***	0.21***
	[0.14]	[0.14]	[0.13]	[0.10]	[0.14]	[0.04]	[0.02]
post-C&T trend break (β_2^p)	-0.43**	-0.44**	-0.42**	-0.28**	-0.45**	-0.43***	-0.43***
	[0.19]	[0.19]	[0.18]	[0.13]	[0.19]	[0.06]	[0.04]
Observations	16,488	16,488	16,488	16,470	16,491	16,488	16,488
Panel d: PM_{10}							
EJ gap:							
pre-C&T trend (β_1^p)	0.22	0.23	0.21	0.12	0.23	0.22***	0.22***
	[0.15]	[0.15]	[0.14]	[0.10]	[0.15]	[0.04]	[0.03]
post-C&T trend break (β_2^p)	-0.48**	-0.49**	-0.46**	-0.31**	-0.50**	-0.48***	-0.48***
	[0.20]	[0.21]	[0.19]	[0.13]	[0.20]	[0.07]	[0.04]
Observations	16,488	16,488	16,488	16,470	16,491	16,488	16,488

NOTES: Estimates of the pre-C&T EJ gap trend (i.e., β_1^p from equation (2)) and post-C&T EJ gap trend break (i.e., β_2^p from equation (2)) for NO_x, SO_x, $PM_{2.5}$, and PM_{10} down panels. All models include zip code-specific and year-specific dummy variables. Observations weighted by zip code-level average population during 2008-2012. Column 1 shows the benchmark model. Column 2 applies a slower pollution decay to HYSPLIT pollution trajectories (i.e., 10% larger half-life parameter). Column 3 applies a faster pollution decay to HYSPLIT pollution trajectories (i.e., 10% smaller half-life parameter). Column 4 applies a lower planetary boundary layer set at 0.5 km. Column 5 applies a higher planetary boundary layer set at 2 km. Column 6 adjusts standard errors for spatial (500 km uniform kernel) and serial correlation (5 years). Column 7 adjusts standard errors allowing correlation across pollutants using a Seemingly Unrelated Regression (SUR) procedure. Standard errors in brackets. P-values from two-sided t-tests with *** p<0.01, ** p<0.05, * p<0.1.

Table S6: Robustness: log exposure

	(1) ln NO_x	(2) ln SO_x	(3) ln $PM_{2.5}$	(4) ln PM_{10}
EJ gap:				
pre-C&T trend (β_1^p)	0.05***	0.04*	0.02	0.02
	[0.02]	[0.02]	[0.01]	[0.01]
post-C&T trend break (β_2^p)	-0.05***	-0.04*	-0.03*	-0.03**
	[0.02]	[0.02]	[0.01]	[0.01]
Zip codes	1650	1650	1650	1650
Observations	16,488	16,480	16,483	16,483

NOTES: Estimates of the pre-C&T EJ gap trend (i.e., β_1^p from equation (2)) and post-C&T EJ gap trend break (i.e., β_2^p from equation (2)) for ln NO_x, ln SO_x, ln $PM_{2.5}$, and ln PM_{10}, across columns. All models include zip code-specific and year-specific dummy variables. Observations weighted by zip code-level average population during 2008-2012. Standard errors clustered at the county-level in brackets. P-values from two-sided t-tests with *** p<0.01, ** p<0.05, * p<0.1.

Table S7: Importance of modeling spatial transport

	(1) Facility zip code	(2) 1.6 km circle	(3) 4 km circle	(4) 2008 transport	(5) 2013 transport	(6) 2017 transport	(7) Full transport
	Panel a: NO_x						
EJ gap:							
pre-C&T trend (β_1^p)	-0.15	0.07	-0.12	-0.09	-0.10	-0.12	0.08
	[0.19]	[0.18]	[0.38]	[0.07]	[0.08]	[0.08]	[0.09]
post-C&T trend break (β_2^p)	0.24	-0.18	0.13	-0.21***	-0.25***	-0.24***	-0.35**
	[0.22]	[0.16]	[0.48]	[0.07]	[0.08]	[0.09]	[0.13]
Observations	1,742	3,825	6,551	16,486	16,483	16,482	16,488
	Panel b: SO_x						
EJ gap:							
pre-C&T trend (β_1^p)	-0.16	-0.08	-0.04	-0.07*	-0.08*	-0.08*	0.10
	[0.10]	[0.09]	[0.14]	[0.03]	[0.04]	[0.04]	[0.09]
post-C&T trend break (β_2^p)	0.18	-0.03	0.00	-0.15***	-0.19**	-0.19**	-0.29**
	[0.12]	[0.09]	[0.19]	[0.06]	[0.08]	[0.09]	[0.14]
Observations	1,644	3,631	6,238	16,486	16,483	16,482	16,488
	Panel c: $PM_{2.5}$						
EJ gap:							
pre-C&T trend (β_1^p)	-0.01	-0.03	-0.15	0.02	0.02	0.02	0.21
	[0.02]	[0.02]	[0.10]	[0.04]	[0.05]	[0.05]	[0.14]
post-C&T trend break (β_2^p)	0.02	-0.02	0.16	-0.27***	-0.32**	-0.35**	-0.43**
	[0.02]	[0.02]	[0.14]	[0.08]	[0.14]	[0.16]	[0.19]
Observations	1,710	3,792	6,501	16,486	16,483	16,482	16,488
	Panel d: PM_{10}						
EJ gap:							
pre-C&T trend (β_1^p)	-0.02	-0.04	-0.16	0.02	0.01	0.01	0.22
	[0.02]	[0.02]	[0.11]	[0.04]	[0.05]	[0.05]	[0.15]
post-C&T trend break (β_2^p)	0.02	-0.03	0.17	-0.30***	-0.36**	-0.39**	-0.48**
	[0.02]	[0.02]	[0.15]	[0.09]	[0.14]	[0.16]	[0.20]
Observations	1,711	3,794	6,502	16,486	16,483	16,482	16,488

NOTES: Estimates of the pre-C&T EJ gap trend (i.e., β_1^p from eq. (2)) and post-C&T EJ gap trend break (i.e., β_2^p from eq. (2)) for NO_x, SO_x, $PM_{2.5}$, and PM_{10} down panels. All models include zip code-specific and year-specific dummy variables. Observations weighted by zip code-level average population during 2008-2012. Column 1 assigns pollution exposure to only the zip code of the emitting facility. Columns 2 and 3 assign pollution exposure to zip codes with centroid within a 1.6 and 4 km circle of emitting facility, respectively. Columns 4-6 assign pollution exposure based on transport pattern only in 2008, 2013, and 2017, respectively. Column 7 reproduces benchmark estimates in panel a of Table 1 using HYSPLIT to fully model pollution transport every 4 hours throughout 2008-2017. Standard errors clustered at the county-level in brackets. P-values from two-sided t-tests with *** p<0.01, ** p<0.05, * p<0.1.

Table S8: Modeling secondary PM$_{2.5}$ exposure using InMAP

	(1) Primary PM$_{2.5}$	(2) Total PM$_{2.5}$
	Panel a: Trend-break model	
EJ gap:		
pre-C&T trend (β_1^p)	-0.004 [0.008]	-0.005 [0.008]
post-C&T trend ($\beta_1^p + \beta_2^p$)	-0.019* [0.010]	-0.024** [0.012]
post-C&T trend break (β_2^p)	-0.015 [0.014]	-0.019 [0.016]
EJ gap pct. change since 2012	47	43
	Panel b: Year-specific effects model	
EJ gap:		
in 2008	0.018 [0.025]	0.026 [0.026]
in 2009	0.019 [0.025]	0.024 [0.026]
in 2010	0.021 [0.025]	0.024 [0.026]
in 2011	-0.001 [0.001]	0.000 [0.001]
in 2012	-	-
in 2013	-0.003 [0.002]	-0.003 [0.002]
in 2014	-0.031* [0.018]	-0.037* [0.021]
in 2015	-0.038* [0.020]	-0.048** [0.024]
in 2016	-0.095** [0.047]	-0.121** [0.057]
in 2017	-0.081* [0.044]	-0.099* [0.052]
Zip codes	1647	1647
Observations	16,470	16,470

NOTES: Panel a shows estimates of the pre-C&T EJ gap trend (i.e., β_1^p from equation (2)), post-C&T EJ gap trend (i.e., $\beta_1^p + \beta_2^p$ from equation (2)), and and post-C&T EJ gap trend break (i.e., β_2^p from equation (2)). Column 1 examines InMAP-modeled primary PM$_{2.5}$ exposure. Column 2 examines inMAP-modeled total (i.e., primary and secondary) PM$_{2.5}$ exposure. PM$_{2.5}$ exposure in average μg/m^3 within a year. InMAP employs transport patterns for 2005 and not for the 2008-2017 sample period. Percentage change in EJ gap calculated between 2012 and 2017. Panel b shows a more flexible version of equation (2) by estimating year-specific EJ gaps with 2012 being the omitted year. All models include zip code-specific and year-specific dummy variables. Observations weighted by zip code-level average population during 2008-2012. Standard errors clustered at the county-level in brackets. P-values from two-sided t-tests with *** p<0.01, ** p<0.05, * p<0.1.